

## SMASIS2011-) % -

### PLANAR RF ANTENNA RECONFIGURATION WITH NI-TI SHAPE MEMORY ALLOYS

P.J. Wolcott\*

M.J. Dapino<sup>†</sup>

Smart Materials and Structures Laboratory  
Department of Mechanical and Aerospace Engineering  
The Ohio State University  
Columbus, Ohio 43210  
Email: dapino.1@osu.edu

Z. Wang<sup>‡</sup>

L. Zhang

Electro-Science Laboratory  
Department of Electrical and Computer Engineering  
The Ohio State University  
Columbus, Ohio 43210  
Email: zhang.471@osu.edu

#### ABSTRACT

Nickel-titanium shape memory alloys (SMA) are utilized to achieve a multi-band RF (radio frequency) antenna through reconfiguration. Switches made from shape memory alloys electronically connect together a planar antenna arrangement, creating several electrical signal pathways and reconfiguration to be realized. The changes in geometry induced by the switching create different working frequencies of the antenna leading to multiple bands. The switches open and close due to an induced phase change from martensite to austenite via resistive heating from a separate electric circuit. Switch design is based on a previously successful switch geometry with the goal of miniaturizing the reconfigurable antenna system. Simulations were performed to determine an optimal geometry for reconfiguration with the switches to generate measurable changes in working frequency in a planar antenna. Based on these simulations, a planar antenna consisting of a dielectric material between conductive copper layers was designed and constructed for use with the SMA switches. The antenna design is based on a patch antenna that is reconfigured to new geometries as the SMA switches are activated. The working frequency of the planar antenna arrangement can be tuned to between 2.25 GHz and 2.43 GHz depending on geometry as measured with  $S_{11}$  signal reflection.

**Keywords:** Shape memory alloys, RF antennas, planar antenna, Ni-Ti.

#### INTRODUCTION

Small, multifunctional radio frequency (RF) devices are critical in commercial and military communications applications. Examples of their use include portable devices for high data rate communications via ground and satellite means; miniature ultra wideband antennas on thin, flexible substrates in Unmanned Aerial Vehicles (UAVs); multifunctional/reconfigurable apertures and many more. These applications are of growing importance and the need to develop these devices for such applications is essential.

To create small, multi-band antennas, reconfiguration within the antenna structure is necessary. Multiple methods have been employed to realize antenna reconfiguration; these methods are based upon changes in material properties or geometry. Changes in material properties create controllable, solid state variations in the electrical properties of the component materials to achieve new operating frequencies. Geometric changes are often achieved through switching mechanisms, such as MEMS (Micro-Electro-Mechanical Systems) devices, that change the signal pathway of the antenna to change the operating frequency. Other switching methods, such as using smart materials, provide a robust technique to create large changes in the operating frequency without significant degradation in antenna performance.

\*Email: wolcott.27@osu.edu

<sup>†</sup>Address all correspondence to this author.

<sup>‡</sup>Email: wang.1460@osu.edu

This method was tested using a simple monopole geometry as well as a planar microstrip transmission line to confirm reconfiguration performance in a planar arrangement [1].

Shape memory alloys (SMAs) provide one way of creating a controllable shape change for antenna reconfiguration. Shape memory alloys can recover an original shape after deformation when heated above the austenitic finish temperature. Specifically, Ni-Ti can withstand up to 8% strain and fully recover its original shape upon heating [2]. Phase transformations of the alloy between martensitic and austenitic phases allows for the large strains that can be recovered with heating [3]. The martensitic phase has a monoclinic structure that can have a twinned or detwinned microstructure. Stress acting on the twinned state rearranges the alternating monoclinic orientations in one direction to form the detwinned phase. Heating causes a phase change to austenite, a cubic crystalline microstructure. Upon cooling, the microstructure returns to the twinned martensitic phase when no stress is applied to the material.

Using the principles of the shape memory effect, a trained shape can be developed that can be recovered with heat [4]. This allows shape memory alloys such as Ni-Ti to be used as actuators without the need for larger, more complicated switching mechanisms [5]. In this way, SMAs can produce a large force per unit volume while operating under a simple mechanism [6]. One specific type of actuator using SMAs is the bias force actuator. This type of actuator uses a bias spring to generate the restoring force in the one way shape memory effect [5]. The SMA begins in the deformed state at low temperature and when heated, deflects a spring that stores the potential energy. When the SMA is cooled, the potential energy stored in the spring is released to strain the SMA to its original, deformed position [5]. This type of actuator can be modified to use an elastic beam as the spring to restore the deformed position.

This study investigates the implementation of Ni-Ti switches in a radiating, planar antenna building upon the principles discovered in [1] to create a robust, reconfigurable front end antenna. The switches use design elements of a bias spring type actuator using an elastic beam as the bias spring. The SMA actuators provide a switching mechanism to create a change in the geometry of the antenna and an associated shift in the working frequency.

## SMA SWITCH DESIGN

Two switches were built for this study using the principles outlined in [1] using a normally open switch configuration. The components of the design for each include a Ni-Ti ribbon on top of a spring steel beam each electrically insulated from one another with Kapton tape. A schematic of the switch design and motion is shown in Fig. 1. In this design, the Ni-Ti strip begins in the detwinned martensitic phase when the switch is “off” and is resistively heated with current to transform into the trained

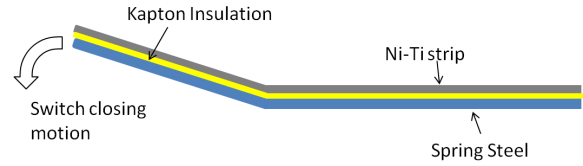


**FIGURE 1.** SCHEMATIC REPRESENTATION OF SWITCH COMPONENTS AND MOTION.



**FIGURE 2.** SCHEMATIC OF NI-TI STRIP CIRCUIT FOR RESISTIVE HEATING

austenitic phase. The Ni-Ti ribbon is split in the center to create an electric circuit where current can flow and resistively heat the Ni-Ti strip as shown in Fig. 2. As the heating and transformation occur, the Ni-Ti strip pushes down on the spring steel until an electrical contact is made with the planar antenna. When the current is turned off, the Ni-Ti strip cools and the spring steel deforms the Ni-Ti strip upward, returning to the detwinned switch “off” state. In this design, the split tails of the Ni-Ti strip are fixed onto the antenna and connected to a power supply while the actuation side of the switch is free to move up and down for reconfiguration. This type of design represents a normally open configuration because when no current is supplied to the Ni-Ti strip, there is no electrical contact with the planar antenna.

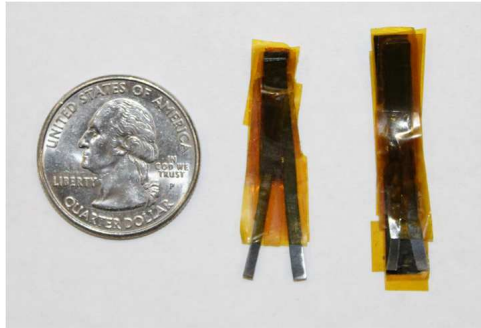
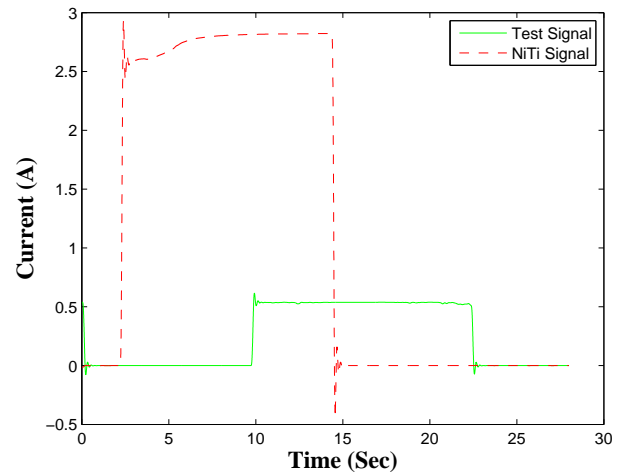
The switch dimensions are given in Table 1, where both Switch A and Switch B are represented. The overall dimensions of the switch are slightly larger than the sum of the Ni-Ti strip and spring steel due to the Kapton insulation. As it is seen in the table, the two switches are of similar size which allows for easier implementation into the planar antenna design. Figure 3 shows an image of the two switches. The transformation temperatures of the Ni-Ti strip used in both switches were measured with differential scanning calorimetry and were found to be:  $A_s = 58^\circ\text{C}$ ,  $A_f = 71^\circ\text{C}$ ,  $M_s = 51^\circ\text{C}$  and  $M_f = 42^\circ\text{C}$ . Each switch is activated via resistive heating with a direct current of 2.75 A.

## SMA SWITCH TESTING

To evaluate the SMA switch actuation, tests were conducted on each switch to ensure they were opening and closing properly. These tests consisted of actuating each switch separately via power supply at 2.75 A and measuring the time it took to close a contact between two copper wires. The copper wires were connected to a separate power supply, producing approxi-

**TABLE 1.** DIMENSIONS OF THE SWITCHES CONSTRUCTED (OVERALL DIMENSIONS INCLUDE KAPTON INSULATION).

	Switch A			Switch B		
	Length (mm)	Width (mm)	Thickness (mm)	Length (mm)	Width (mm)	Thickness (mm)
Ni-Ti	33.8	3.5	0.254	33.5	3.5	0.254
Spring Steel	22.2	3.5	0.127	35.5	5.3	0.127
Overall	33.8	5.6	0.762	36.1	6.8	0.762

**FIGURE 3.** IMAGE OF THE TWO SWITCHES USED (SWITCH A LEFT, SWITCH B RIGHT).**FIGURE 4.** SWITCH A: ELECTRICAL CURRENT TEST MEASURING TIME TO OPEN/CLOSE CIRCUIT UPON HEATING/COOLING

mately 0.5 A current. Copper tape was placed on the actuating tip of the SMA switches for electrical conduction and the current in each circuit was measured. Once contact was made between the switch and the copper wires, the resistive heating of the SMA was turned off and the time for the switch to actuate upwards, breaking the circuit, was measured.

Figures 4 and 5 show the actuation cycles for each of the switches. The Ni-Ti signal represents the current heating the SMA switch while the test signal represents the copper wire test circuit. When the current is on in the test circuit there is contact between the SMA switch and the copper wire. It can be seen that the opening and closing of the contact for switch A takes approximately 8 sec. while switch B closes contact in approximately 8 sec. and opens the circuit in approximately 15 sec. Differences in actuation between the two switches are attributed to the slight differences in their geometries. The times for actuation can be optimized by altering the current used for heating and/or supplying air to remove heat more quickly, however these factors were not included in these experiments. Based on these tests, the switch actuation for each SMA switch is confirmed as working properly.

## PLANAR ANTENNA DESIGN

A planar reconfigurable antenna was designed to incorporate the built switches, using HFSS full-wave electromagnetic field simulation software [7]. The detailed antenna design is shown in Fig. 6. The design consists of a main patch 54 mm x 40 mm in size with two segments 21.3 mm x 1 mm unattached to the main segment. For this design, the switches are placed on the antenna such that in the “on” state, the switches mechanically deform and contact the two segments below the main patch antenna creating reconfiguration. Electrical connection is established between the segments and the main patch, resulting in an effective increase in the antenna dimensions. The locations of both switches are chosen to ensure an optimized impedance match is achieved when the switches are on. As a result, compared to the “off” state, an “on” antenna is effectively larger in dimensions, with a decreased characteristic resonance frequency.

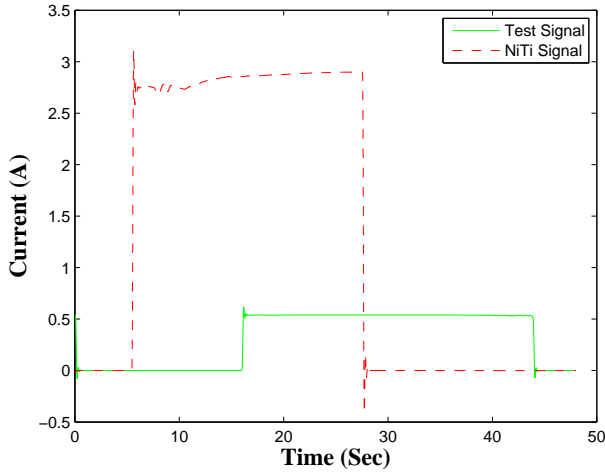


**FIGURE 5. SWITCH B: ELECTRICAL CURRENT TEST MEASURING TIME TO OPEN/CLOSE CIRCUIT UPON HEATING/COOLING**

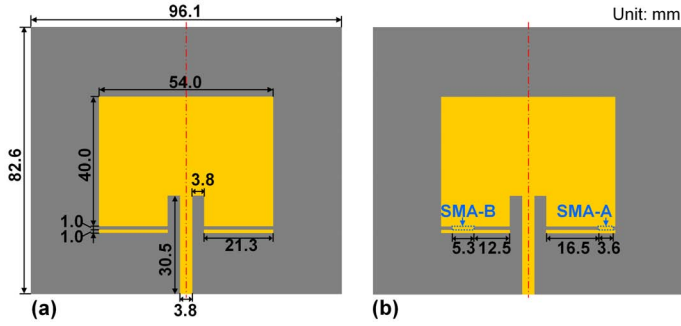


**FIGURE 6. RECONFIGURABLE PATCH ANTENNA DIMENSIONS (A) SWITCHES OFF, (B) SWITCHES ON CONNECTING TWO SEGMENTS WITH MAIN PATCH ANTENNA.**

## ANTENNA CONSTRUCTION AND SWITCH IMPLEMENTATION

The antenna pattern was fabricated by laser milling a copper layer cladded onto a Duroid 5880 dielectric substrate ( $\epsilon_r = 2.2$ ,  $\tan \delta = 0.0009$ , thickness = 1.575 mm) with a copper ground plane.

Figure 7 shows a schematic side view of the antenna with a switch for reconfiguration between the main patch portion of the antenna and the unconnected segment. Copper tapes were placed on the actuating end of the switches to provide an optimal electrical contact between the antenna and the “on” switches.

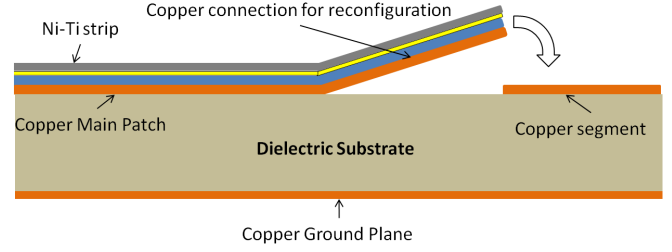


**FIGURE 7. SIDE VIEW SCHEMATIC OF SWITCH MECHANISM OPENING AND CLOSING FOR RECONFIGURATION**

## ANTENNA TESTING

To test the antenna reconfigurability, the resonance frequency and reflection coefficient ( $S_{11}$ ) of each possible configuration was measured using a network analyzer (Agilent N5242A, PNA-X). The four configurations tested included both switches “off”, one switch connecting the left segment, one switch connecting the right segment and both switches connected simultaneously; each configuration can be seen in Fig. 8. For the switch “on” configurations, the tail portion of the switches were fixed to the main patch antenna while the actuating end of the switch connected the segment to the main patch.

All four antenna configurations are shown in Fig. 8 along with corresponding measurement results for  $S_{11}$  in each of the configurations. When both switches were “off”, the resonance was observed at 2.43 GHz. Since the switch design is a normally open arrangement, the configuration with both switches “off” provides a baseline for antenna performance when no reconfiguration is attempted. When only switch A or B was “on”, only one segment was connected to the main antenna. This created larger antenna dimensions, and a lower resonance occurred at 2.32 GHz or 2.31 GHz respectively. Finally, when both switches were “on”, both segments were connected to the antenna. The effective antenna size further increased and the resonance shifted down to 2.25 GHz. The maximum frequency shift from both switches “on” to “off” was 180 MHz. It is also noteworthy that for all four configurations, the  $S_{11}$  was lower or close to 10 dB. This indicates that the reflected power was less than or close to 10%, which is satisfactory for a working antenna.

The difference between the resonance frequencies in each of the one switch “on” geometries is due to the slight difference in switch dimensions between switch A and switch B. This can be seen in Fig. 8 (b) and (c) where the  $S_{11}$  results are slightly asymmetric due to the small dimensional variations between the two switches.

Furthermore, the measured antenna performance matched well with the results of the simulations. Figure 9 shows the data of the configurations with both switches “on” and “off”. The small discrepancies seen are attributed to measurement error where a slight mismatch of the reconfiguration geometry could

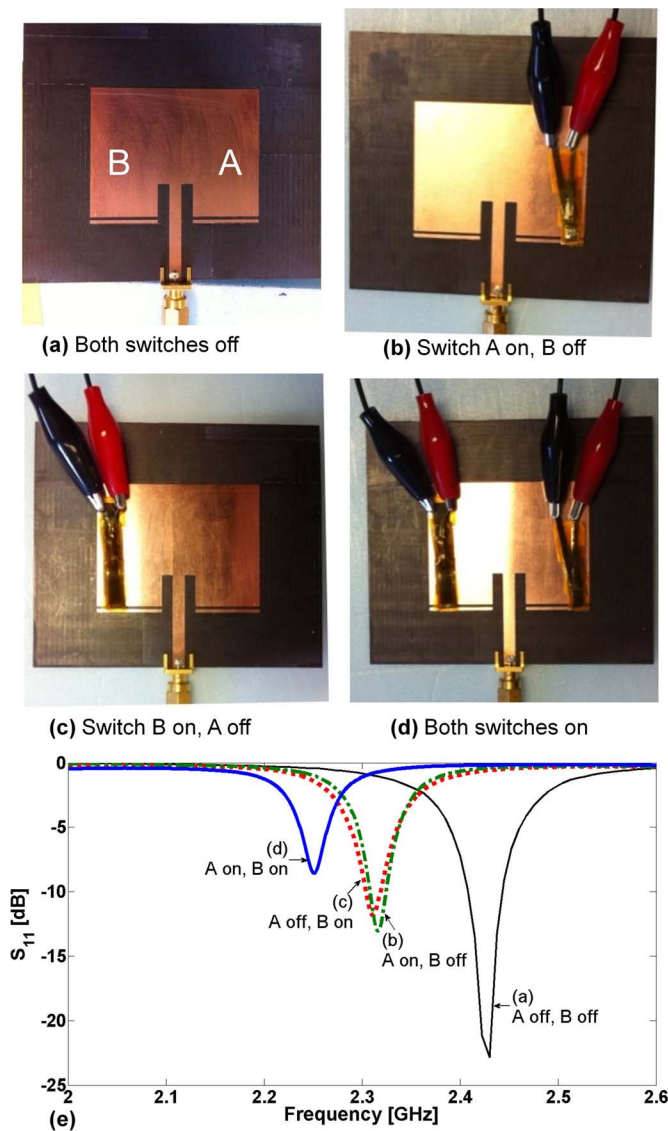


**FIGURE 8.** (A-D) FOUR ANTENNA CONFIGURATIONS USING SWITCHES ON AND/OR OFF (E) MEASURED  $S_{11}$  AND CHARACTERISTIC RESONANCE FREQUENCY FOR EACH CONFIGURATION (A-D).

lead to small changes in the resonance frequency and  $S_{11}$  measurement.

## CONCLUSIONS AND FUTURE WORK

Using shape memory alloy switches has proven successful in creating multiple configurations within a planar antenna structure to change the working frequency of the device. The multiple configurations were achieved by activating the switches into an

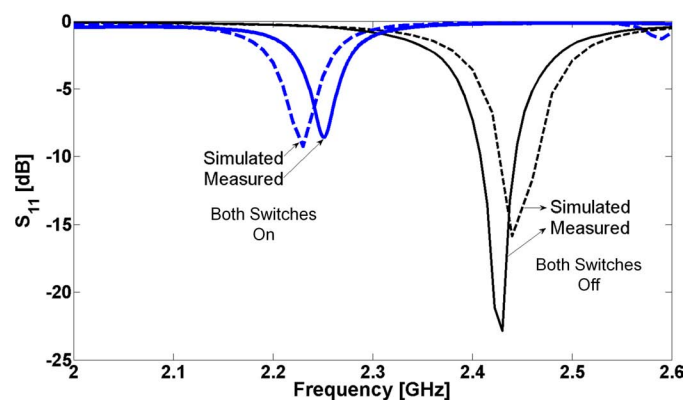


**FIGURE 9.** COMPARISON OF MEASUREMENT AND SIMULATED ANTENNA PERFORMANCE WITH BOTH SWITCHES ON AND OFF.

“on” or “off” position, creating varying signal pathways for the antenna. The varying geometries caused by the switching created changes in the working frequency making the overall structure multi-band in nature. The various frequencies are shown to be tunable based on simulations of the geometry of the device. Re-configuration of the planar antenna led to a maximum shift in the resonance frequency of 180 MHz from the change in geometry produced by the activation of both switches.

To further prove the viability of shape memory alloy switches for reconfiguration in planar antenna devices, several areas must be addressed. Firstly, the gain and radiation pattern of the antenna with the various geometries must be measured. The gain measurements are necessary to determine all potential applications for this reconfigurable antenna. Next, depending on the application for these switches, it may be necessary to further miniaturize the switches to reduce the amount of current necessary for actuation. Existing switch geometries require 2.75 A for resistive heating which could be problematic for smaller aeronautical applications such as UAVs which may not have a large power source available for antenna operations. Lowering the required current would also include a further investigation of the electrical circuit used to heat the device.

## ACKNOWLEDGMENT

The authors would like to thank Dr. John Volakis of the OSU Electro-Science Laboratory for assistance with this work. Financial support for this research was provided by the OSU Institute for Materials Research Interdisciplinary Materials Research Grant, the Ohio Space Grant Consortium, and the Smart Vehicle Concepts Center ([www.SmartVehicleCenter.org](http://www.SmartVehicleCenter.org)), a National Science Foundation Industry/University Collaborative Research Center.

## REFERENCES

- [1] Wolcott, P.J, Dapino, M.D. and Zhang, L., 2011, “Smart Switch Metamaterials for Multiband Radio Frequency Antennas,” *Journal of Intelligent Material Systems and Structures*, **To appear**.
- [2] Davis, J.R., 2003, *Handbook of Materials for Medical Devices*, ASM International.
- [3] Lagoudas, D., 2008, *Shape Memory Alloys*, Science and Business Media, LLC.
- [4] Kai,Y. and Chengin G., 2002, “Design and Control of Novel Embedded SMA Actuators,” *Journal of Electrical and Electronics Engineering*, **22**, pp. 513-520.
- [5] Liang, C. and Rogers, C.A., 1997, “Design of Shape Memory Alloy Actuators,” *Journal of Intelligent Material Systems and Structures*, **8**303, pp. 303-313.
- [6] Kim, H.C., Yoo, Y.I. and Lee, J.J., 2008, “Development of a NiTi actuator using a two-way shape memory effect induced by compressive loading cycles,” *Sensors and Actuators A: Physical*, **148**, pp. 437–432.
- [7] Balanis, C.A., 2005, *Antenna Theory: Analysis and Design*, Wiley-Interscience.